RADIOMETRIC CALIBRATION OF THE MASTCAM-Z CAMERAS FOR MARS2020 A. G. Hayes[1], P.M. Corlies[1], C. Tate[1], M. Barrington[1], J.F. Bell III[2], J.N. Maki[3], A. Winhold[2], E. Jensen[4], M.A. Ravine[4], M.A. Caplinger[4], K.M. Kinch[5], K. Herkenhoff[6], J. Johnson[7], M. Rice[8], B. Horgan[9], O. Busborg[5], B. Ehlman[10],J. van Beek[3], G. Parr[11], P. Caballo-Perucha[11];[1]Cornell University, Ithaca NY, [2]ASU, Tempe AZ, [3]JPL, Pasadena CA, [4]MSSS, San Diego CA [5]Univ. of Copenhagen, Denmark, [6]USGS, Flagstaff AZ, [7]JHU/APL, Laurel MD, [8]Western Washington Univ., Bellingham WA, [9]Purdue, South Bend IN, [10]Caltech, Pasadena CA, [11]Joanneum Research, Graz Austria

Abstract: Data acquisition for stand-alone radiometric calibration of the Mars2020 Mastcam-Z instrument was conducted in April and May of 2019. We describe a summary of testing and derived instrument performance, focusing on temperature-dependent effects discovered and characterized during testing.

Overview: The Mast Camera Zoom (Mastcam-Z) instrument on the NASA Mars 2020 rover consists of a pair of zoomable CCD cameras with filter wheels that can acquire multispectral (400–1000 nm), stereoscopic images of the Martian surface and atmosphere at focal lengths from 26-110 mm. Externally mounted calibration targets enable in-flight relative reflectance calibration and two electronics boards within the rover body enable data processing and transmission to the spacecraft's central computer. The cameras are mounted 2 m above ground level atop a mast that enables 360° rotation in azimuth and ±90° in elevation.

The primary goals of Mastcam-Z preflight radiometric testing were to characterize system performance over a range of relevant environmental conditions, validate models of instrument performance to permit interpolation/extrapolation to conditions where preflight testing was not possible, and to acquire data sufficient to enable the conversion of measured Data Number (DN) to an accurate estimate of incidence in physical units ($Wm^{-2}sr^{-1}$ or ph $s^{-1}m^{-2}sr^{-1}$ integrated over filter bandpasses).

Each of the radiometric tests performed during stand-alone calibration were targeted at understanding a coefficient in the camera equation that converts reported DN to physical units, specifically the radiance (W $m^{-2}sr^{-1}$) impinging upon the front aperture of the instrument. Camera response (*DN*) is proportional to the incoming radiance at the front aperture (*L*), weighted by the spectral response (*r(λ)*) of the instrument:

$$DN_{ijkl} = \frac{A_o \Omega_l (t + t_{sm,ij})}{g F_{ijkl}} r_{o,k} \int \overline{r}_k L(\lambda) d\lambda + B_{ij} + D_{ij} t$$

where DN_{ijkl} is the 12-bit digital-number of pixel (*i,j*) using filter *k* at zoom position *l*. $A_o\Omega_l$ [m^2sr] is the optical efficiency, defined as the product of the effective collecting area and instantaneous field of view (IFOV) at zoom setting *l*. *g* [e^-/DN] is the detector gain , *t* [s] is the exposure time, and t_{sm} [s] is a filter-dependent additional exposure time that accounts for inefficient charge clearing and shutter smear in the detector. $r_{o,k}$ is the bayer-dependent radiometric coefficient for filter *k*, while $\overline{r}_k(\lambda)$ is the normalized spectral profile that describes the system's weighted spectral response (incorporating optical transmission, filter response, and detector quantum efficiency). $L(\lambda)$ [W $m^{-2}sr^{-1}nm^{-1}$] is the radiance incident upon the front aperture. B_{ij} [DN] is the static bias, D_{ij} [e^-/s] is the dark current, and F_{ij} is the flat-field coefficient required to make pixel (*i,j*) behave like the average of the central 200x200 pixels.

Stand-alone calibration was performed at ambient conditions in a class 10000 clean room at Malin Space Science Systems (MSSS) in San Diego, CA. Each of the coefficients in the camera equation were determined using a calibrated integrating sphere and monochromator. A subset of testing was performed inside a vacuum chamber at MSSS at temperatures ranging from -50°C to 0°C. Observed temperature-dependent effects were characterized in further detail using a commercial-off-the-shelf Mastcam-Z Analog Spectral Simulator (MASI) [1], which uses flight spare filters and the same detector as Mastcam-Z. MASI's detector is packaged within a Joule-Thomson cooler that permits temperature control between -50°C and +50°C.

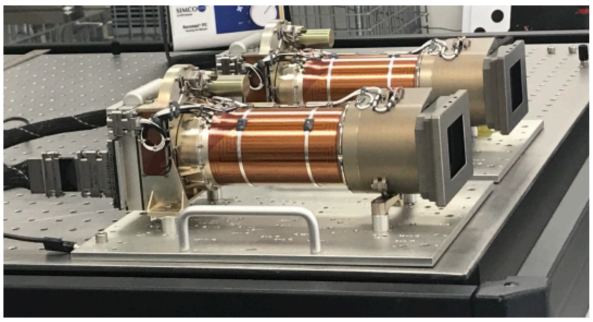

Figure 1: Image of the Mastcam-Z cameras on an optical bench at MSSS during stand-alone calibration.

Summary of Results: While *g*, $A_o\Omega_l$, t_{sm}, F_{ijkl}, and $\overline{r}_k$ were observed to be temperature-independent, r_o, D_{ij}, and B_{ij} varied with focal plane temperature. Despite its temperature dependence, D_{ij} is small (< 48 e^-/s at Mars-relevant temperatures) and B_{ij} / t_{sm} can be removed by acquiring a zero-exposure frame before or after a science image for which radiometric accuracy is required.

Integrating sphere images at multiple temperatures were acquired to determine the CCD gain, read noise, and full well using the photon transfer technique as described in Janesick et al. 1987 [2]. We find that the gain (*g*) of each camera agrees to within error with a value of 16±0.1 e^-/DN. Read noise (*RN*) and full-well also agreed, with values of 21±2 e^-, and 21000 e^-, respectively. While *g* and *RN* were not found to vary with temperature, full-well increased to 25000 e^- when temperatures were dropped from ambient to -5°C.

For a circular aperture, optical efficiency ($A_o\Omega_i$) can be recast in terms of f-number ($f_\#$) and pixel area (A_D) $\left(A_o\Omega_i = (\pi A_D)\left(4f_{\#,i}^2\right)^{-1}\right)$. While most parameters of the camera equation are independent of zoom (e.g., *g*, $r_{o,k}$), the $f_\#$ is not. Optical $f_\#$ was found by observing constant illumination over a range of zoom positions while all other camera parameters were held fixed. Derived *f#* values were anchored to vendor-provided data at 100 mm effective focal length (efl, $f_{\#,100mm}$=9.1) and found to vary between 7 and 9.65 for efls between 26 mm and 110 mm, respectively. This same dataset was used to derive flat field coefficients (F_{ijkl}) at 67 zoom positions for *R0/L0*. These flat fields accommodated optical effects resulting from changing zoom (e.g., vignetting) and were combined with flat fields derived for each filter at three zoom positions (3, 68, and 100 mm) that provided high frequency pixel-to-pixel response variations found to be independent of zoom and temperature.

System spectral throughput ($\overline{r}_k(\lambda)$) was measured using a monochromator with a slit width set to a spectral divergence of ~2 nm (Figure 2). Normalized spectral response was measured only at ambient conditions, but testing with MASI has confirmed that normalized spectral profiles show no observable temperature dependence. The observed spectral profiles were combined with observations from a calibrated integrating sphere to derive radiometric coefficients for each filter ($r_{o,k}$). Testing conducted in an MSSS vacuum chamber found that, integrated across the spectral bandpass, these coefficients do show a measureable temperature dependence. Testing with MASI confirmed the magnitude of the temperature dependence and discovered it was larger for the infrared filters and not noticeable at shorter wavelengths (see Table 1). Analysis of Mars Science Laboratory data confirm that Mastcam [3] has the same temperature dependence, but that conversion to *I/F* reflectance using the on-board calibration target can remove it as long as the calibration target images are acquired under similar conditions to the to-be-calibrated images. Temperature dependence was reported as the relative slope of the radiometric coefficient with temperature (B=$\Delta r_{o,k}/\Delta$T), and can lead to variations as high as 43% between -50 to +5°C for filter *R6* (1017±18 nm).

References: [1] Barrington et al. (2019) *LPSC* [2] Janesick et al. 1987 *SPIE* [3] Bell et al. (2017) *Earth & Space Sci.*

Filter	Wavelength [nm]	HWHM [mn]	Beta [1/C]
L0 (Red)	634	43	0.0010
L0 (Green)	542	42	0.0005
L0 (Blue)	476	46	0.0001
L1	801	9	0.0021
L2	754	10	0.0018
L3	677	11	0.0014
L4	605	9	0.0008
L5	528	11	0.0002
L6	442	12	-0.0001
L7	590	88	0.0008
R0 (Red)	634	43	0.0010
R0 (Green)	542	42	0.0005
R0 (Blue)	476	45	0.0001
R1	800	10	0.0021
R2	866	10	0.0028
R3	910	12	0.0039
R4	939	13	0.0042
R5	978	10	0.0054
R6	1017	18	0.0078
R7	880	10	0.0031

Table 1: Effective Wavelength, Half-Width-Half-Maximum (HWHM), and relative temperature response (B=$\Delta r_{o,k}/\Delta$T) for each Mastcam-Z filter.

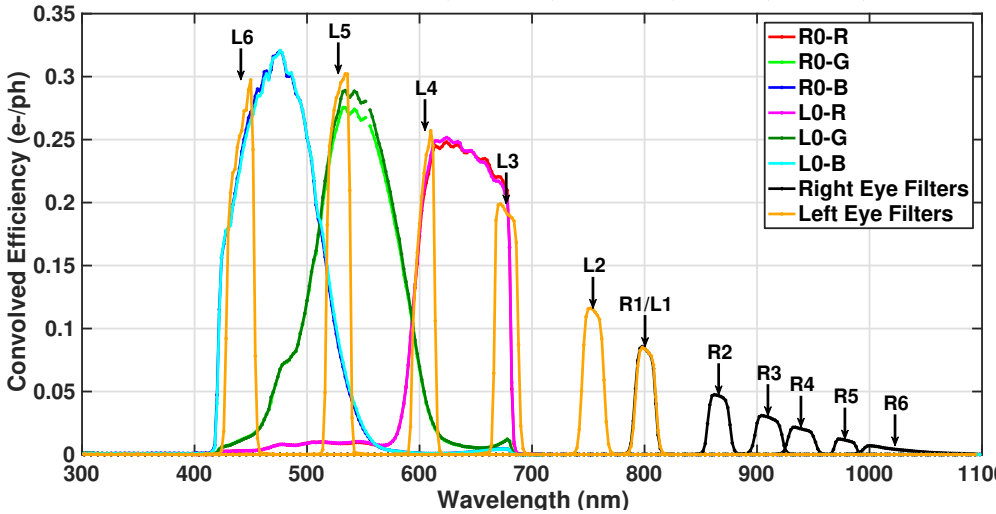

Figure 2: Weighted spectral response (e^-/ph) of the Mastcam-Z cameras for filters R0-R6 and L0-L6 at 100 mm effective focal length.